

Measurement of Yield Strength and Flow Properties In Spot Welds and Their HAZs at Various Strain Rates

F.M. Haggag
Advanced Technology Corporation
Oak Ridge, TN

G. E. C. Bell
Oak Ridge National Laboratory
Oak Ridge, TN

ABSTRACT

A portable/in-situ stress-strain microprobe was developed to evaluate the integrity of metallic components [including base metal, welds, and heat-affected-zones (HAZs)]. The microprobe system utilizes an automated ball indentation (ABI) technique to determine several key mechanical properties (e.g., yield strength, true-stress/true-plastic-strain curve, strain-hardening exponent, Luders strain, and elastic modulus). This paper describes ABI test results, from several welds and their HAZs, using the patented microprobe system developed recently at Advanced Technology Corporation. A bench-top configuration of the microprobe system was used successfully to test spot welds in 1020 ferritic steel and 2219 aluminum sheets at various strain rates.

INTRODUCTION

The ABI test is based on strain-controlled multiple indentations (at the same penetration location) of a polished surface by a spherical indenter (0.25 to 1.57 mm diameter). The patented microprobe turn-key system and test method (1) are based on physical and

mathematical relationships which govern metal behavior under multiaxial indentation loading. Good agreement (less than 5%) has been obtained between ABI-derived data and those from conventional ASTM methods (1-7).

A summary of the ABI test technique is presented in another paper by Haggag in the proceedings of this conference (2), and more details are given elsewhere (3-7). The microprobe system utilizes an electro-mechanically-driven indenter, high resolution penetration transducer and load cell, a personal computer (PC), a 16-bit data acquisition/control board, and ABI software. Automation of the test, where a 386 PC and test controller were used to control the test (including a real-time graphic and digital display of load-depth test data) as well as to analyze test data (including tabulated summary and macro-generated plots), made it simple, rapid, accurate, and highly reproducible. Results of ABI tests (at several strain rates) on various base metals, welds, and HAZs, at different metallurgical conditions are presented and discussed in this paper.

Test materials included resistance spot welds and their HAZs in: (a) 1020 ferritic steel sheets

(1.25 mm-thick) tested at slow and high strain rates, and (b) 1.00 mm-thick sheets of 2219 aluminum tested at slow strain rates. Different amounts of heat input were used in the resistance spot welds to simulate variations during industrial resistance spot welding in automobiles and appliances. Gradients in the yield strength and flow properties and correlations to the material microstructure in the weld and HAZ areas are discussed.

RESULTS

The spot welds were sectioned and mounted in epoxy with the joined sheets covering the full height of the mount, hence, low mount compliance did not affect the test results when indenting the base metal, HAZ, and weld nugget areas. The specimens were also etched so that the HAZ width became apparent for positioning the indents. ABI tests were conducted using a 0.508 mm diameter tungsten carbide ball indenter at indenter speeds from 0.003 to 0.127 mm/s. Fig. 1 shows a sample of a spot weld with two indents made in the base metal and one each in the weld nugget and in the HAZ area.

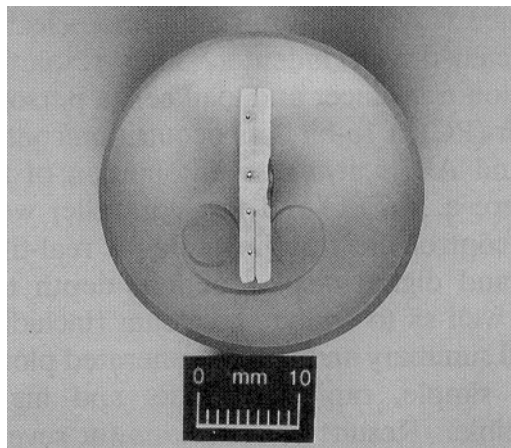
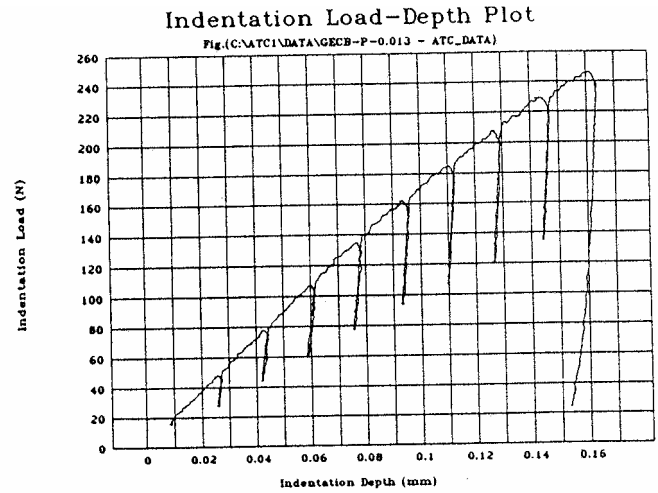


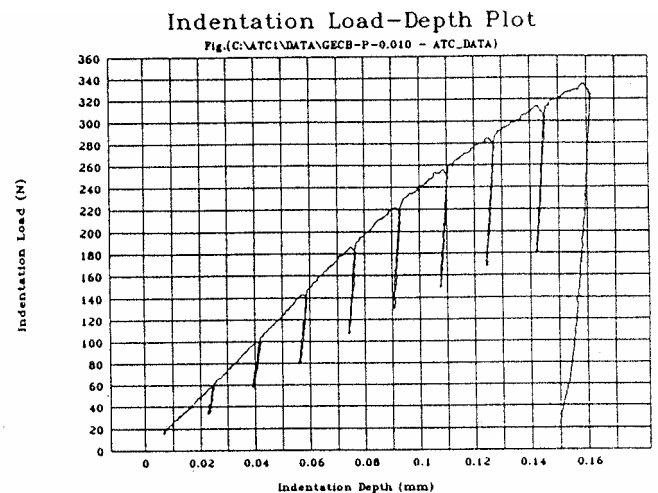
Fig. 1 Mounted 1020 Steel Spot Weld.

A sample of the indentation load-depth plots is shown in Fig. 2 (a) and (b) for the base metal and the weld nugget of the 1020 steel. It can be seen that for the same maximum

indentation depth (approximately 0.16 mm), the maximum load was approximately 245 and 330 N for the base metal and weld nugget, respectively. This is consistent with the higher yield strength and flow properties (True-stress/true-plastic-strain curve) for the carbon steel material.



Base Metal, 1020 Steel, Specimen E, Test No. 13



Weld Nugget, 1020 Steel Spot Weld, Specimen E, Test No. 10

Fig. 2 Indentation Load-depth data of 1020 steel: (a) base metal (b) weld nugget.

The yield strength is calculated from all indentation cycles. During ball indentation at each penetration depth (load cycle), new (fresh) material yielding and work hardening occur simultaneously with increasing volume as the

ball indenter penetration depth is increased. This is in contrast to the uniaxial tensile test where the volume of the gage section of the tensile specimen is constant, and hence, the 0.2% offset yield strength is calculated from a single measurement past the elastic behavior. Fig. 3 shows a sample of the yield strength calculation plot. The value of the indentation load (P) divided by the square of the chordal diameter of the indentation (d') when the latter equals the indenter diameter (D) is termed the specimen material parameter (A). The ABI-derived yield strength is calculated by multiplying "A" by the material's yield coefficient (an empirical value of 0.2285 for carbon steels, and 0.219 for aluminum alloys).

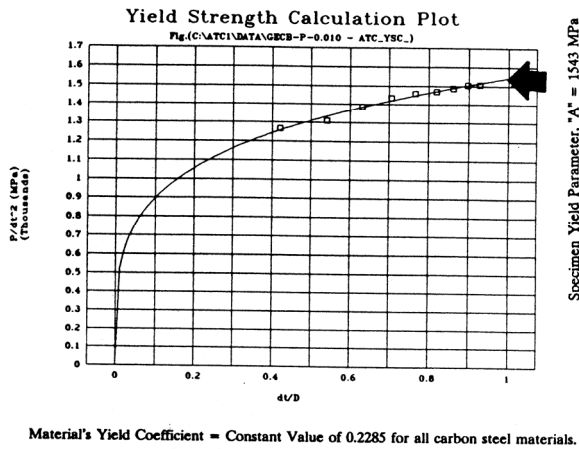


Fig. 3 Yield strength plot for 1020 steel specimen 1020-E weld nugget.

The true-stress/true-plastic-strain data are obtained from the equations described in another paper by Haggag in this conference (2) and more details are given elsewhere (3-7). A sample of ABI-derived stress-strain curve of the weld nugget of a 1020 steel specimen is shown in Fig. 4. The data were fitted to a power law according to ASTM standard E 646 for determining the strain-hardening exponent (n). The true-stress (σ_t)/true-plastic-strain (ϵ_p) curve can be represented by the following power law equation:

$$\sigma_t = K \epsilon_p^n$$

Where

n = strain-hardening exponent,
K = strength coefficient

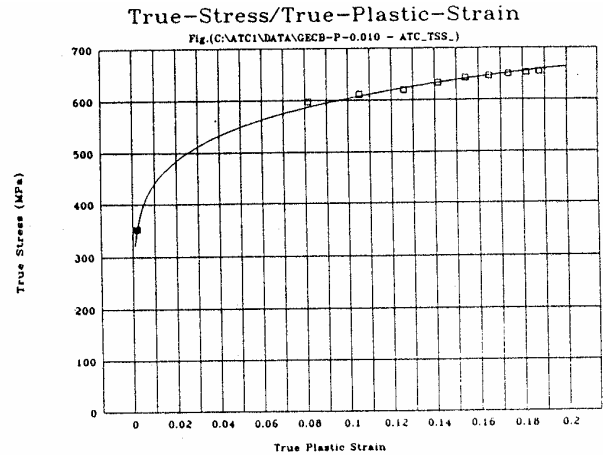


Fig. 4 ABI-measured flow properties for weld nugget specimen No. 1020-E.

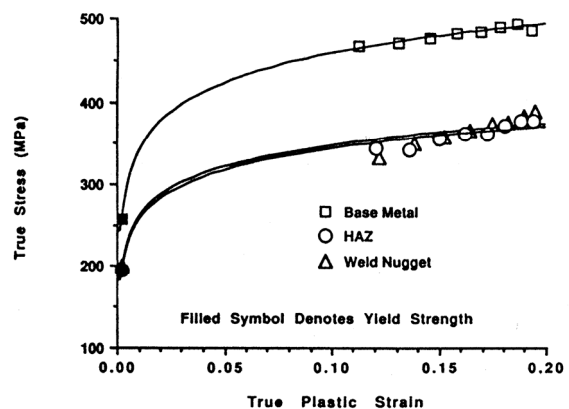
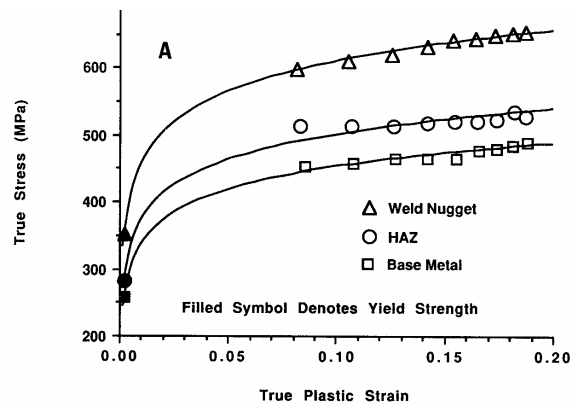


Fig. 5 Example of ABI test results on spot welds: (a) 1020 steel and (b) aluminum.

An example of the $\sigma_t-\epsilon_p$ curves for the base metal, HAZ, and weld nugget for the spot welds of the two materials is shown in Fig. 5 (a) and (b). This figure shows that the weld nugget and HAZ curves are higher than the base metal for the 1020 carbon steel while the weld and HAZ stress-strain curves were lower than the aluminum base metal. The ABI test results on the resistance spot welds are summarized in Table 1.

DISCUSSION

Material 1020 is a solid solution iron-carbon alloy while 2219 is a precipitation strengthened aluminum alloy. During resistance spot welding/heating/quenching, martensite or bainite precipitation increases the strength of the weld nugget and HAZ relative to the base metal of 1020 steel (see microstructure in Fig. 6). For 2219 aluminum, heating during resistance spot welding dissolves precipitates and reduces the strength of the nugget and HAZ relative to the base metal. (Note clean microstructure in the center of weld nugget of 2219 as compared to precipitation structure in base metal (Fig. 7).

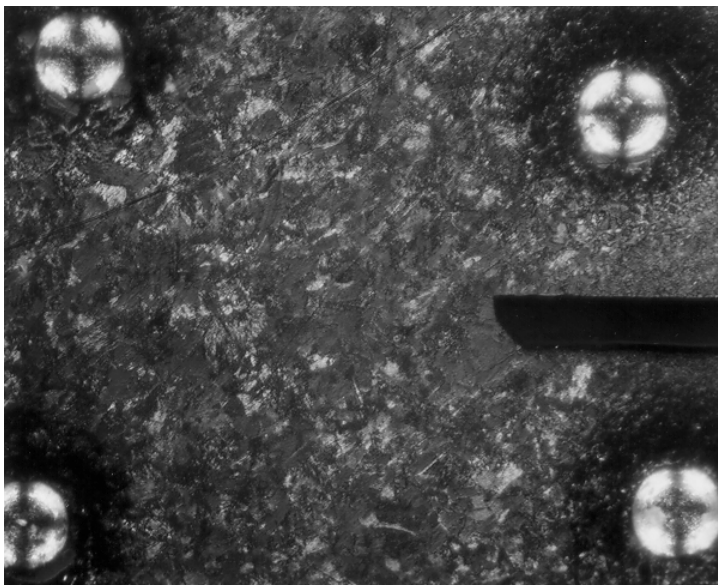
All ABI tests in Table 1 were conducted at an indenter speed of 0.006 mm/s. However, increasing the strain rate by a factor of 40 (changing the indenter speed from 0.003 to 0.127 mm/s) resulted in small increases (5-10%) in the strain-hardening exponent (n) and the strength coefficient (K) of weld nuggets of 1020 steel spot welds. The effect of strain rate on yield strength and flow properties is very important for determining the integrity of spot welds in automobiles during crash accidents.

The percentage increase in yield strength of weld nugget and HAZ relative to the base metal in 1020 steel is higher for smaller spot welds because of higher quenching rate and hence increased precipitation and strength.

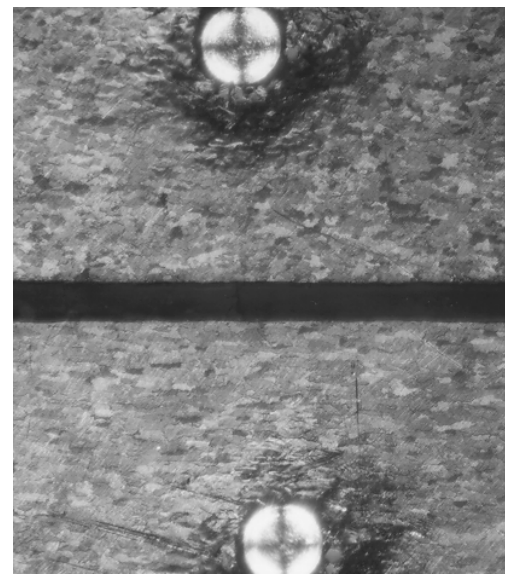
CONCLUSION

The ABI technique was very successful in accurately measuring the yield strength and flow properties of spot welds in thin sheets of 1020 mild steel and 2219 aluminum alloy at different strain rates.

The mechanical properties of HAZ and weld nuggets were higher than the base metal in 1020 mild steel spot welds while they were



(a) Weld nugget



(b) Base metal.

Fig. 6 Microstructure of spot weld.

Table 1. SUMMARY OF YIELD STRENGTH AND FLOW PROPERTIES RESULTS
FROM ABI TESTING OF 1020 STEEL AND 2219 ALUMINUM

Material/Location	σ_y (MPa)	$\Delta\sigma_y/\sigma_y^{BM}$	K (MPa)	N (= ϵ_u)	σ_{UTS} (MPa)
1020 Mild Steel, Small Spot Weld (1020-B)					
Base Metal	223		540.1	0.142	359
HAZ	345	(54.7%)	829.1	0.139	553
Weld Nugget	421	(88.8%)	1007.4	0.138	673
1020 Mild Steel, Medium Spot Weld (1020-C)					
Base Metal	225		563.9	0.147	371
HAZ	297	(32.0%)	755.1	0.146	497
Weld Nugget	386	(71.6%)	938.0	0.140	624
1020 Mild Steel, Large Spot Weld (1020-E)					
Base Metal	254		613.4	0.141	408
HAZ	281	(10.6%)	685.7	0.141	456
Weld Nugget	353	(39.0%)	826.8	0.137	554
2219 Aluminum Spot Weld					
Base Metal	253		634.3	0.147	417
HAZ	184	(-27.3%)	432.3	0.138	289
Weld Nugget	191	(124.5%)	444.0	0.136	298

Where:

σ_y = Yield Strength

σ_y^{BM} = Yield Strength of Base Metal

K = Strength Proportionality Constant

n = Strain-hardening-exponent

ϵ_u = Uniform elongation

σ_{UTS} = Engineering Ultimate Strength = $(K n^n)/(1 + n)$



(a) Weld nugget



(b) Base Metal

Fig. 7 Microstructure of 2219 Al spot weld.

lower than the base metal in 2219 aluminum alloy. The ABI test results were consistent with the type of alloy and its microstructure, and the resistance spot welding conditions.

ACKNOWLEDGMENT

This work was partially supported by Office of Fusion Energy, U.S. Department of Energy, under contract DE-AC05-84OR21400 with Martin Marietta Energy Svstems. Inc.

REFERENCES

1. Haggag, F. M., U.S. Patent No. 4,852,397, August 1, 1989.
2. Haggag, F. M., "Application of Flow Properties Microprobe to Evaluate Gradients in Weldment properties," Proceedings of the ASM 3rd International Conference on Trends in Welding Research, 1-5 June 1992, Gatlinburg, Tennessee, 1993.
3. Haggag, F. M., Wong, H., Alexander, D. J., and Nanstad, R. K., Proceedings of the 2nd Conference on "Trends in Welding Research," May 14-18, 1989, Gatlinburg, Tennessee, pp. 843-849.

4. Haggag, F. M., Nanstad, R. K., Hutton, J. T., Thomas, D. L., and Swain, R. L., Application of Automation Technology to Fatigue and Fracture testing, ASTM STP 1092, Braun, A. A., Ashbaugh, N. E., and Smith, F. M., Eds., American Society for Testing and Materials, Philadelphia, 1990, pp. 188-208.
5. Haggag, F. M., Nanstad, R. K., and Braski, D. N., pp. 101-107 in Innovative Approaches to Irradiation Damage and Failure Analysis, D. L. Marriott, T. R. Mager, and W. H. Bamford, Eds., PVP Vol. 170, American Society of Mechanical Engineers, New York, 1989.
6. Haggag, F. M. and Nanstad, R. K., pp. 41-46 in Innovative Approaches to Irradiation Damage and Failure Analysis, D. L. Marriott, T. R. Mager, and W. H. Bamford, Eds., PVP Vol. 170, American Society of Mechanical Engineers, New York, 1989.
7. Haggag, F. M., "In-situ Measurements of Yield Strength and Flow Properties Using A Novel ABI System," presented at the ASTM Symposium on Small Specimen Test Techniques and Their Application to Nuclear reactor Vessel Thermal Annealing and Plant Life Extension, New Orleans, Louisiana, January 1992, to be published in an ASTM STP.